Sensing membrane stress with near IR-emissive porphyrins

Neha P. Kamat[a], Zhengzheng Liao[b], Laurel E. Moses[a], Jeff Rawson[c], Michael J. Therien[c], Ivan J. Dmochowski[b,1], and Daniel A. Hammer[a,d,1]

[a]Department of Bioengineering, University of Pennsylvania, 210 South 33rd Street, 240 Skirkanich Hall, Philadelphia, PA 19104; [b]Department of Chemistry, University of Pennsylvania, 231 South 34th Street, Philadelphia, PA 19104; [c]Department of Chemistry, Duke University, 124 Science Drive, Durham, NC 27708; and [d]Department of Chemical and Biomolecular Engineering, University of Pennsylvania, 220 South 33rd Street, Philadelphia, PA 19104

Edited by Shu Chien, University of California at San Diego, La Jolla, CA, and approved July 14, 2011 (received for review February 7, 2011)

Probes embedded within a structure can enable prediction of material behavior or failure. Carefully assembled composites that respond intelligently to physical changes within a material could be useful as intrinsic sensors. Molecular rotors are one such tool that can respond optically to physical environmental changes. Here, we propose to use molecular rotors within a polymersome membrane to report membrane stress. Using supermolecular porphyrin-based fluorophores as rotors, we characterize changes in the optical emission of these near-infrared (NIR) emissive probes embedded within the hydrophobic core of the polymersome membrane. The configuration of entrapped fluorophore depends on the available space within the membrane; in response to increased volume, emission is blue shifted. We used this feature to study how shifts in fluorescence correlate to membrane integrity, imparted by membrane stress. We monitored changes in emission of these porphyrin-based fluorophores resulting from membrane stress produced through a range of physical and chemical perturbations, including surfactant-induced lysis, hydrolytic lysis, thermal degradation, and applied stress by micropipette aspiration. This paper comprehensively illustrates the potential for supermolecular porphyrin-based fluorophores to detect intrinsic physical changes in a wide variety of environments, and suggests how molecular rotors may be used in soft materials science and biology as sensors.

fluorescent stress sensor | rheology | soft matter

Development of internal-strain sensors can enhance our ability to monitor material stability and predict material failure. Mechano-optical molecules have great potential as intrinsic sensors because of their ability to report their molecular environment with high spatial and temporal resolution. Several probes, including mechanophores (1) and quantum dots (2), have recently been developed to detect local stress changes in polymeric materials. The technological applications of such sensors range from soft materials science to biology. For example, embedded sensors could be used in rheology as a reporter of local stresses within complex multilength scale composites under flow. Furthermore, embedded composites could be used to track the progress of an internalized vesicle within a cell, as a monitor of drug delivery. Choi et al. (2) recently demonstrated the potential of using emission wavelength shifts from embedded luminescent probes to detect localized stresses in polymeric fibers. Using a probe that can both noncovalently incorporate into materials and continuously monitor material properties without requiring external interference to reset sensing capabilities would advance both the versatility and responsiveness of local stress sensors. Despite these advances, a sensor that is nontoxic in biological environments, reports physical changes in its environment with large emission wavelength shifts, and can easily be incorporated into larger materials without compromising the mechanical properties, remains to be developed.

Fluorescent molecular rotors are molecules that sensitively detect changes in their physical environment. These molecules have the ability to internally rotate, opening or closing a nonradiative relaxation pathway, which influences fluorescence emission. The twisting motion within a rotor is influenced by local environmental changes or stresses that aid or inhibit internal rotation. Traditionally, molecular rotors have been used as viscosity probes (3–5), detecting changes in local shear stress, temperature, and membrane fluidity. This sensitivity to physical environmental changes indicates that molecular rotors can be used more broadly to sense changes in material cohesion and stability as well. Recently, porphyrin-based molecular rotors have gained interest due to their potential for functionalization and incorporation into more complex structures (6, 7). In addition, meso-to-meso ethyne-bridged (porphinato)zinc(II) oligomers (PZn_n compounds) investigated by Duncan et al. (8) demonstrate exceptional near-infrared (NIR) fluorescence, furthering their potential as in vivo stress probes.

Here, we use these PZn_n supermolecular fluorophores as reporters of membrane stability. The porphyrin oligomers used in this study, structurally shown in Fig. 1*A*, exhibit structural heterogeneity in solution that derives primarily from the low barrier to rotation about the meso-to-meso ethyne bridge. This low barrier causes a torsional angle distribution between the planar PZn components of these structures. In solution, following electronic excitation, PZn_n fluorophores exhibit relaxation dynamics that diminish the mean PZn-PZn torsional angle, producing a more conformationally uniform, highly planarized emissive state (9, 10). Conformationally restrictive environments can reduce PZn_n ground-state torsional angle distributions relative to those manifest in solution, as well as the extent to which these species may undergo excited-state structural relaxation to produce more uniform and planarized emissive states. For example, PZn_n fluorophores that possess more planar ground-state conformations and reside in environments that augment rotational barriers between juxtaposed porphyrin macrocycles will exhibit red-shifted emission relative to that observed in solution. Because PZn_n emission wavelength is intimately correlated with molecular conformation, we can use fluorescence measurements to quantify changes in the structure and integrity of the supermolecule's membrane environment.

Polymersomes, vesicles in which the membrane is assembled from block copolymers, are ideal materials for hosting a conformationally dependent stress sensor in that the available membrane volume can be precisely controlled by changing both

Author contributions: N.P.K., Z.L., I.J.D., and D.A.H. designed research; N.P.K., Z.L., and L.E.M. performed research; J.R., M.J.T., and I.J.D. contributed new reagents/analytic tools; N.P.K. and Z.L. analyzed data; and N.P.K., Z.L., M.J.T., I.J.D., and D.A.H. wrote the paper.

The authors declare no conflict of interest.

This article is a PNAS Direct Submission.

[1]To whom correspondence may be addressed. E-mail: ivandmo@sas.upenn.edu or hammer@seas.upenn.edu.

This article contains supporting information online at www.pnas.org/lookup/suppl/doi:10.1073/pnas.1102125108/-/DCSupplemental.

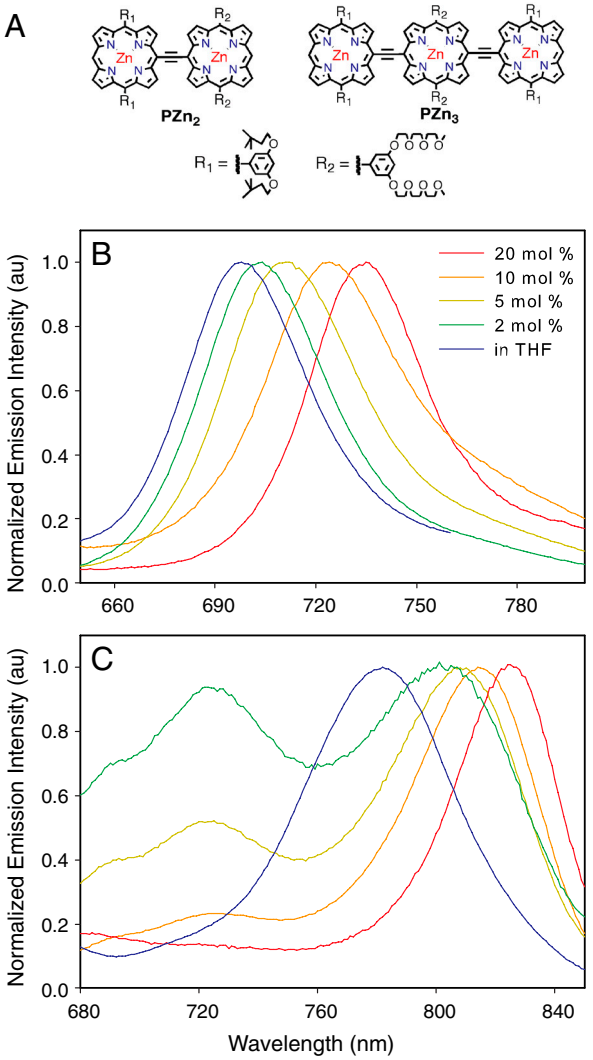

Fig. 1. Spectral range of porphyrin-based fluorophore emission. (*A*) Structures of the meso-to-meso ethyne-bridged (porphinato)zinc(II) dimer (PZn_2) and trimer (PZn_3). (*B*) PZn_2 exhibits an emission maximum at 699 nm (blue) in THF; this emission maximum is dependent upon its concentration in the polymersome membrane, and ranges up to 735 nm (red) in 3,800 M_r PEO-b-PBD polymer membranes at 20 mol % loading. (*C*) PZn_3 exhibits an emission maximum at 787 nm (blue) in THF; this emission maximum shifts bathochromically with increasing concentration in the polymersome membrane and ranges up to 825 nm (red) in PEO-b-PBD polymer membranes at 20 mol % loading. Emission spectra obtained for polymersomes loaded with PZn_2 and PZn_3 at concentrations of 2, 5, and 10 mol % are shown, respectively, in green, yellow, and orange.

PZn_n concentration and the polymer molecular weight. Furthermore, these bilayer membranes are models for cellular membranes. In this manuscript, we show that PZn_n fluorophores structurally respond to reductions in conformational space by reducing their PZn-PZn torsional angle; we further correlate the corresponding PZn_n emission wavelength shifts that result from physical changes in polymersome membranes induced through surfactant, hydrolytic, thermal, and mechanical stimulus.

Results and Discussion

Steady-State Porphyrin Emission as a Function of Membrane Dispersion. The structural and spectroscopic properties of a wide variety of PZn_n-based emissive polymersomes have been reported (11–15). These studies, for example, correlated the observed emissive properties with PZn_n concentration and structure, as a function of the nature of fluorophore spatial confinement within the polymer membrane (14). It was shown that incorporating PZn_n fluorophores into polymersomes at concentrations up to 10 mol % does not compromise the mechanical stability (critical aerial strain, polymer chain packing, and interfacial aqueous/membrane phenomena) of the vesicle assemblies (12). Because these studies characterize: (*i*) how $\mathbf{PZn_n}$ structure and concentration impacts emission wavelength, emission intensity, and energy-transfer dynamics within membrane environments (14, 15), (*ii*) how the nature of the membrane-forming polymer impacts $\mathbf{PZn_n}$ emissive properties (13), (*iii*) how $\mathbf{PZn_n}$ structural characteristics and concentration impact membrane mechanical stability (12), and (*iv*) how fluorophore structure dictates $\mathbf{PZn_n}$ spatial distribution within a membrane (14), these emissive moieties define ideal probes of physical changes to membrane environments.

Polymersomes were made from the amphiphilic diblock copolymer poly(ethyleneoxide)-b-poly(butadiene), PEO_{30}-*b*-PBD_{46} ($M_r = 3{,}800$ Da). PZn_n fluorophores were entrapped within the hydrophobic core of the membrane during assembly; these species included a dimer, PZn_2 ($M_r = 2{,}123$ Da) and a trimer, PZn_3 ($M_r = 3{,}071$ Da).

Both PZn_2 and PZn_3 demonstrate emission spectra with maxima that vary with solvent and concentration in polymersomes; previous studies demonstrate that these fluorophores are dispersed within the polymersomal bilayer in a spatial domain defined at the junction of the hydrophobic PBD and hydrophilic PEO polymer blocks (14). PZn_2 exhibits an emission maximum at 699 nm (blue) in THF; in 3,800 M_r PEO-b-PBD-based polymersome membranes, the emission maximum progressively red-shifts from 705 to 735 nm (red) as PZn_2 loading increases from 2 to 20 mol % (Fig. 1*B*). Likewise, PZn_3, which exhibits an emission maximum at 787 nm in THF solvent, displays a progressive emission band maximum red-shift from 805–825 nm as its loading within the polymersomal bilayer increases from 2 to 20 mol % (Fig. 1*C*). These spectral red-shifts of PZn_n fluorophores as a function of increasing polymersome membrane concentration have previously been shown to derive from increasingly narrower PZn-PZn torsional angle distributions centered about an increasingly diminished mean macrocycle-macrocycle torsional angle (13–15). Although membrane volumes remain constant, the available volume for fluorophore dispersion can change. As polymersome PZn_n concentration increases, increased ordering of polymer chains drives a progressive reduction of fluorophore structural heterogeneity, resulting in increasingly more uniform and more planarized structures.

Kuimova et al. (7) recently utilized a ratiometric approach to determine the average, steady-state conformation of a porphyrin-based rotor in a cell, in which the most red-shifted and blue-shifted emission maxima that were observed were assigned, respectively, to the planar and twisted conformations. For a given emission spectrum, the ratio of these emission intensities quantifies these respective conformational populations. Following this method, fluorescence intensity ratios determined at emission maxima of 735/699 nm (PZn_2) and 825/787 nm (PZn_3) were utilized to characterize the relative populations of more planarized and more twisted PZn_n fluorophores. Characterizing PZn_n conformation with a ratiometric method proves more sensitive at detecting changes in porphyrin conformation than using emission peak wavelengths (Fig. S1*A*). This ratiometric approach was used to calibrate PZn_2 conformational distributions in standard viscosity solutions of methanol/glycerol (Fig. S1*B*). In accordance with theory (16), the more planar/more twisted emission intensity ratio for PZn_2 scales linearly with viscosity on a double logarithmic scale.

The relative populations of more planarized and more twisted PZn_n conformations as a function of increased concentration in polymersome membranes was next studied by constructing polymer membranes ($M_r = 3{,}800$ Da) containing these fluorophores at loadings ranging from 1 to 10 mol %. Increased concentrations

of PZn_2 or PZn_3 in polymersomes results in increasingly red-shifted fluorescence maxima (Fig. 2*A* and Fig. S2). These data show that the percentage of fluorophores that exist in more planarized structures characterized by a reduced mean PZn-PZn torsional angle is enhanced with increasing concentration. The ratiometric approach also allows for comparison of the extent of concentration-dependent conformational shifts exhibited by PZn_2 and PZn_3. Within the polymersome membrane, PZn_3 adopts more planar conformations at lower concentrations than PZn_2. The larger PZn_3 exerts a greater ordering influence on polymer chains that form the bilayer due to the smaller available dispersion volume at any given fluorophore concentration relative to that for PZn_2.

Changing the Available Membrane Volume. The effect of available membrane volume for dispersion of fluorophores on PZn_2 and PZn_3 conformation was also studied by increasing the hydrophobic core thickness of polymersome membranes. Emissive polymersomes were formed with the diblock copolymer PEO_{80}-*b*-PBD_{125} ($M_r = 10{,}400$ Da). This higher molecular weight polymersome has a larger hydrophobic core thickness (~14.8 nm) than 3,800 M_r polymersomes (~9.6 nm), and therefore, a larger volume available for porphyrin encapsulation (17). Consistent with the above results and analysis, increasing the available membrane volume for dispersion reduces the PZn_n conformational population having planarized structures (Fig. 2*B*). At low fluorophore concentrations where PZn_n molecules are relatively physically unrestricted due to larger PZn_n-PZn_n separation distances (14), PZn_n conformation is predominately dictated by the interaction with the polymer membrane. The intensity ratios of both PZn_2 and PZn_3 converge at low concentrations (≤1 mol %) within polymersomes made from the same diblock copolymer. When interactions with polymer chains dictate fluorophore conformation, longer PEO_{80}-PBD_{125} polymer chains (18), which have more extensive van der Waals interactions and are unable to accommodate fluorophore structural heterogeneity as well as polymersomes based on PEO_{30}-*b*-PBD_{46} chains, cause a higher planar/twisted intensity ratio. In contrast, at high fluorophore concentrations, the extent of PZn_n structural heterogeneity is dominated by the impact of the supermolecular membrane solute upon the nature and degree of polymer-polymer interactions within the bilayer; high PZn_n loading levels drive increased ordering of polymer chains which in turn necessitate reduced fluorophore structural heterogeneity and more uniform and more planarized PZn_n structures.

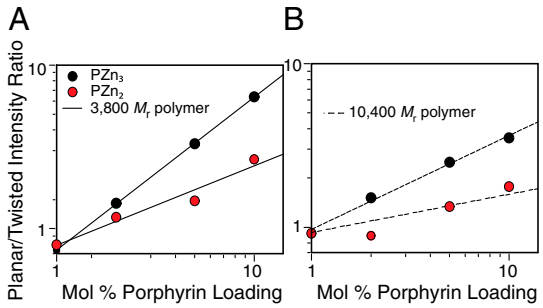

Fig. 2. Effect of PZn_n fluorophore loading and membrane polymer on emission wavelength and intensity. (*A*) Increasing concentrations of PZn_2 (red) or PZn_3 (black) in 3,800 M_r PEO-b-PBD membranes leads to a linear increase in the fraction of fluorophores in more planarized states, as plotted on a double logarithmic scale. For a given sample emission spectrum, the ratio of emission intensities determined at λ_{planar} to $\lambda_{twisted}$ provides a measure of PZn_n structural heterogeneity and the PZn-PZn torsional angle distribution (PZn_2, $\lambda_{planar} = 735$ nm and $\lambda_{twisted} = 699$ nm; PZn_3, $\lambda_{planar} = 825$ nm and $\lambda_{twisted} = 787$ nm). (*B*) Increasing the polymer molecular weight and thus membrane volume with 10,400 M_r PEO-b-PBD membranes leads to a decrease in the fraction of both PZn_2 and PZn_3 in the more planarized state characterized by a reduced mean PZn-PZn torsional angle compared to 3,800 M_r polymer membranes. Linear fits on the double logarithmic scale give R^2 values of (*A*) 0.99 for PZn_3 and 0.99 for PZn_2 and (*B*) 0.97 for PZn_3 and 0.96 for PZn_2.

Characterization of porphyrin conformation in controlled polymer environments demonstrates the sensitive relationship between PZn_n conformation, PZn_n emission, and available membrane volume. When PZn_n fluorophores experience increased conformational volume in the membrane, the fluorophores adopt a more twisted conformation that can be detected by the resulting blue-shifted emission spectra and a reduced planar/twisted intensity ratio. Similarly, when the available volume of the fluorophores is reduced, both PZn_n molecules adopt a more planar conformation with red-shifted emission.

Monitoring Membrane Deformation and Degradation. We set out to show that PZn_n conformation can be used to detect physical changes within a polymer membrane resulting from environmental changes. In cases where the available volume for the fluorophore should be increased by membrane degradation, we expect that PZn_n emission should correspondingly shift to that consistent with more twisted conformations. Membrane degradation was studied in cases of surfactant-induced lysis, hydrolytic degradation, and thermal disruption.

Triton X-100 is a surfactant commonly used to lyse both polymer and cellular membranes. Various concentrations of Triton X-100 were incubated with 3,800 M_r polymersomes containing 10 mol % PZn_2. The more planar/more twisted intensity ratio (735/699 nm) of these NIR-emissive polymersome samples was monitored over time through steady-state fluorescence measurements. As shown in Fig. 3*A*, the emission intensity ratio decreases as the membrane is lysed, indicating an increase in the mean PZn-PZn torsional angle and PZn_2 structural heterogeneity. Increasing the amount of surfactant in solution with polymersomes increases both the rate and the extent of PZn_2 emission blue shift driven by augmentation of the mean PZn-PZn torsional angle.

Vesicles made from biodegradable and bioresorbable polymers have wide appeal for in vivo use as they can facilitate both sustained release of therapeutic drugs and imaging (19, 20). Polymersomes made through self assembly of the diblock copolymer polyethyleneoxide (PEO)-b-polycaprolactone (PCL) hydrolytically degrade at the PCL block ester linkage (21). Although these Food and Drug Administration (FDA)-approved polymers have demonstrated in vivo drug delivery and imaging capabilities (22–25), the ability to track degradation of these vesicles would provide a valuable tool for monitoring in vivo delivery of vesicle encapsulates noninvasively.

Polymersomes made with the biodegradable polymer PEO_{2k}-*b*-PCL_{12k} were assembled with 2 mol % PZn_3. Vesicles were incubated at 37 °C and steady-state emission spectra were collected intermittently over the course of 3 wk. PZn_3 emission spectra exhibited a blue shift, a decrease in intensity, and an increase in spectral breadth as the polymersome membranes degraded and the porphyrin was exposed to an increasingly aqueous environment (Fig. 3*B*). In cases where the fluorophore environment changes in polarity, emission spectra and the corresponding FWHM, maximum intensity, and peak wavelength information, may provide more comprehensive spectroscopic handles with which to track membrane degradation than ratiometric methods alone.

Changes in porphyrin emission were tracked in polymersome membranes undergoing thermally induced rupture. Recently, photoresponsive polymersomes were designed that deform and rupture in response to brief exposure to visible light (400–700 nm) (26, 27). The mechanism of membrane rupture was hypothesized to originate from localized heat production from the predominant nonradiative deexcitation pathways of the PZn_n fluorophores. Thermal expansion of the membrane in this region

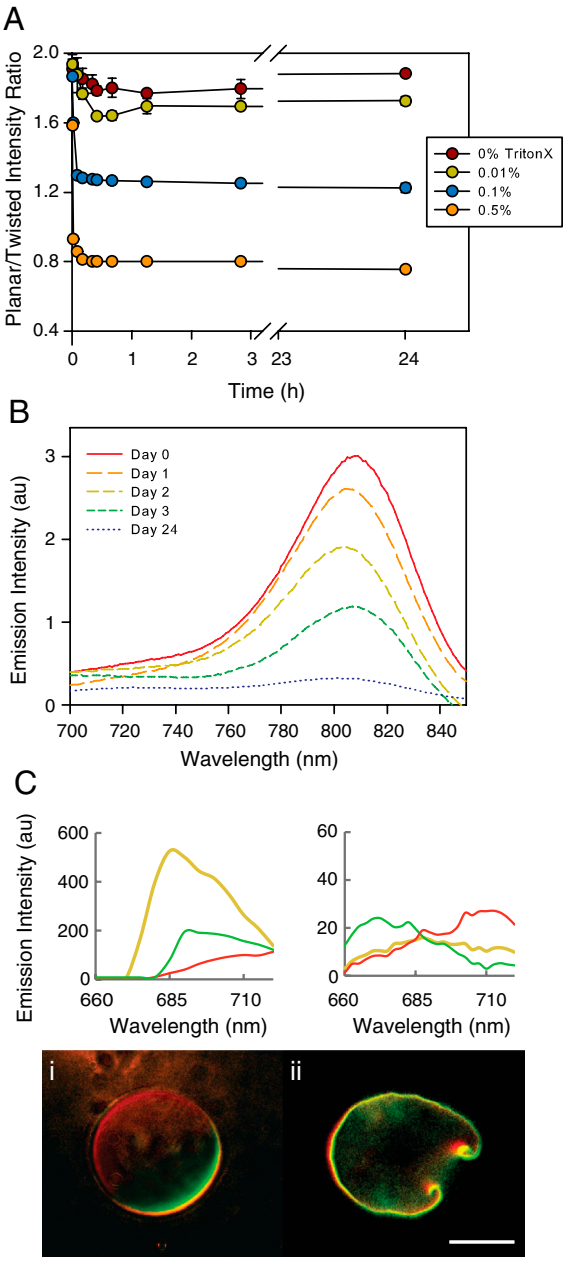

Fig. 3. Porphyrin-based fluorophore emission shifts observed during membrane degradation. (*A*) Triton X-induced lysis leads to a decrease in the more planar/more twisted emission intensity ratio of PZn_2 ($I_{735\,nm}/I_{699\,nm}$). The rate of the observed shift as well as the total fraction of PZn_2 in more twisted conformations increases with the amount of Triton X-100 added to the vesicles. (*B*) Hydrolytic degradation of biodegradable PCL-b-PEO vesicles at 37 °C leads to a decrease in emission intensity, a blue shift of the PZn_3 emission maximum, and an increase in spectral breadth reflecting increased fluorophore strucutral heterogeneity. (*C*, *i*) Localized disruption in photoactive polymersomes leads to increased membrane fluidity in a region of the membrane (lower right of the vesicle) which results in a PZn_2 fluorescence blue shift at this location, highlighted by the green and yellow coloration of the membrane-localized emission. (*ii*) Membrane rupture subsequently occurs at the point of membrane failure 5 min after light exposure. Scale bar is 10 μm.

leads to membrane rupture. This mechanism was confirmed through use of a multispectral imaging system attached to an inverted fluorescence microscope. PZn_2 emission from a single polymersome was collected over a range from 660 to 720 nm (3-nm step size); conformation-dependent emission spectra were resolved through spectral unmixing with Nuance software (method shown in Fig. S3). As shown in Fig. 3*C*, extensive PZn_2 spectral heterogeneity was observed, with one region of the membrane exhibiting blue-shifted emission. The blue-shifted PZn_2 emission indicates an area of increased membrane fluidity that occurs upon localized heating. In the next frame, membrane rupture was observed in the same region. Monitoring the nature of polymersome emission, and thus PZn_n conformation, provides a metric for monitoring membrane stability. In the latter case of thermally induced membrane rupture, single point defects in a membrane can be elucidated through use of multispectral imaging and PZn_n fluorophores.

Instability in membranes can also occur as a result of membrane stress. Micropipette aspiration techniques, developed by Evans et al. (28, 29), provide a method to exert controlled forces on single cell or vesicle membranes. Provided the membrane is fluid, the applied pressure results in a uniformly imposed tension in the vesicle membrane. To determine if porphyrin-based fluorophores could detect applied tension in polymersome membranes, PZn_2-loaded polymersomes were aspirated. Evaluation of PZn_2 emission spectra with a hyperspectral camera indicates that PZn_2 fluorescence blue shifts in response to increasing membrane tension (Fig. 4*A* and Fig. S4*A*). Polymersomes loaded with Nile Red, however, emit light at a constant wavelength regardless of applied stress (Fig. S4*B*).

To confirm the relationship between PZn_2 emission changes and membrane tension, we employed a second method to assess spectral shifts. Light in distinct PZn_2 spectral regions, which reflect the relative populations of more twisted and more planar conformations, was collected using band-pass filters (methods described in Fig. S5 *A*–*B*). For individual, tensed polymersomes, the twisted/planar intensity ratio of embedded PZn_2 ($690 \pm 10/730 \pm 10$ nm) increased linearly with membrane tension (Fig. 4*B*). Controls to ensure that mechanical stress significantly contributes to the PZn_2 fluorescence shift are shown in Fig. S6. The shift of the PZn_2 torsional angle distribution to more twisted geometries implies that the available membrane area is increased in response to increasing membrane tension. This increase in membrane area contrasts with osmotic stress, where hydrophobic volume in the membrane can decrease because of perpendicular stress across the membrane and PZn_2 fluorescence correspondingly red-shifts (Fig. S7). Because aspiration of vesicle membranes in high-tension regimes (>0.5 dyne/cm) results in areal expansion of the membrane, it makes sense that the available area for embedded fluorophores increases. Fig. 4*C* displays the effect of membrane area dilation on PZn_2 conformation, which occurs in response to increasing applied tension. The linear relationship between PZn_2 intensity ratio and membrane areal expansion confirms that imposed membrane tension is reported by porphyrin-based fluorophores by way of increased conformational volume for the fluorophore. We found the rate of change of the PZn_2 intensity ratio in response to membrane tension to be fairly consistent for several tested polymersomes (Fig. 4*D*). These data demonstrate that the fluorescence intensity ratio of each polymersome increases linearly with increasing membrane tension. To better visualize the slopes of the membrane tension versus intensity ratio curves, the plots were adjusted so that the best fit line for each curve passed through the origin. The consistent relationship between change in intensity ratio and change in membrane tension indicates that changes in PZn_2 emission spectra provide a metric for measuring changes in membrane tension.

Conclusion

We show that porphyrin-based PZn_n supermolecular fluorophores emit light sensitively in response to available conformational volume in polymersome membranes. Changes in the available volume for PZn_n accompany local viscosity changes brought about by membrane stress and instability. These molecular rotors can sensitively detect these local material changes with large emission

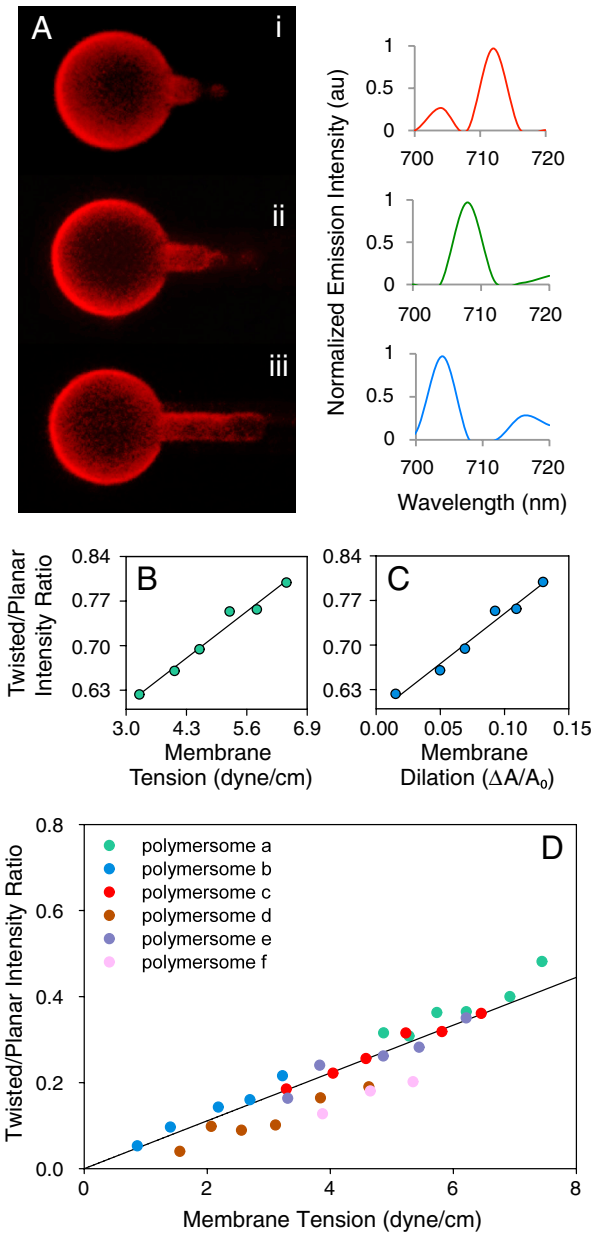

Fig. 4. Micropipette aspiration causes a blue shift of PZn_2 emission. (*A*) Aspiration of a polymersome membrane into a micropipette results in a blue shift of PZn_2 emission in response to the applied membrane stress. Increasing the tension in the polymersome membrane from (*i*) 0.8 dyne/cm to (*ii*) 1.7 dyne/cm to (*iii*) 4.7 dyne/cm, causes embedded porphyrin fluorophores to shift emission to shorter wavelengths. Scale bar is 30 μm. (*B*) The fraction of PZn_2 fluorophores in a twisted state linearly increases in response to increasing membrane tension. The ratio of emission intensities at $\lambda_{twisted} = 690$ nm to $\lambda_{planar} = 730$ nm was determined using a PMT and 730 ± 10 nm and 690 ± 10 nm band-pass emission filters. (*C*) Applied tension through aspiration causes a lateral areal expansion of the membrane and results in a porphyrin blue shift for embedded PZn_2 fluorophores. The increase in membrane area that occurs upon aspiration of the polymersome scales linearly with the increase of fluorophores in the twisted state. Linear fits give R^2 values of (*B*) 0.97 and (*C*) 0.98. (*D*) The adjusted 690/730 nm intensity ratios for several polymersomes undergoing aspiration are plotted. The increase in PZn_2 intensity ratio with applied tension occurs at a similar rate, as demonstrated by the similar slopes of intensity ratio vs. tension curves. The average slope, calculated from the best-fit line of each polymersome, is displayed on the chart.

wavelength shifts. A ratiometric intensity approach allows for sensitive detection of changes in membrane stability brought about by surfactant, hydrolysis, temperature, and mechanical stress. This technique allows real-time monitoring of both membrane deformation and failure. Our study suggests that PZn_n molecular rotors, dispersed in polymersome membranes, can also be used to directly monitor intrinsic physical changes in the porphyrin environment in real time. Given the highly polarized nature of PZn_n electronically excited states, and the established dependence of excited lifetime upon conformation for these fluorophores, fluorescence lifetime imaging microscopy and experiments that probe the evolution of excited-state anisotropy with time will provide complimentary means of assessing membrane stability. Synthetic and biological bilayered vesicles that disperse PZn_n fluorophores define a powerful tool for monitoring rheology and stability of soft matter and biological systems.

Materials and Methods

Vesicle Preparation. Giant (>1 μm diameter) vesicles were prepared as described previously (27). The resulting polymersome membranes contained either PZn_2 or PZn_3 at the molar ratios corresponding to their copolymer-porphyrin solutions.

For experiments involving the biodegradable nanosized vesicles, the diblock copolymer, polyethyleneoxide-b-polycaprolactone (PEO_{45}-*b*-PCL_{105}) was used.

Viscometry. Methanol/glycerol mixtures were prepared by varying methanol, glycerol ratios (vol/vol) from 100% methanol to 100% glycerol. Porphyrin and DMSO were added to the resulting solutions to make 7×10^{-6} M PZn_2 viscosity standards containing 2.8% DMSO. Viscosity measurements were performed using an AR200ex rheometer (TA Instruments) with a 20 mm steel parallel-plate geometry with a 500 mm gap.

Fluorometry. Fluorometry was performed at 25 °C using a Spex Fluorolog-3 spectrophotometer (Jobin Yvon Inc.) that uses a dual S- and T-channel configuration and photomultiplier tube (PMT)/InGaAs/Extended-InGaAs detectors with an excitation wavelength of 480 nm. Single excitation and emission apertures were set to 5 nm.

Determination of Fluorophore Conformation. Ratiometric methods were utilized to characterize the relative populations of more planarized and more twisted PZn_n fluorophores. Fluorescence intensity ratios determined at emission maxima of 735/699 nm (PZn_2) and 825/787 nm (PZn_3) were utilized to characterize the relative populations of more planarized and more twisted PZn_n fluorophores (see text for details). Emission spectra and peak emission wavelengths were used to characterize fluorophore conformational distribution during multispectral imaging studies with PZn_2.

Polymersome Degradation. Lysis experiments were conducted with PEO_{80}-*b*-PBD_{125} polymersomes embedded with 10% PZn_2. Triton X-100 was added to polymersome samples at concentrations ranging from 0.01 to 0.5%. To perform osmotic stress tests, PEO_{80}-*b*-PBD_{125} polymersomes, with 5 mol % PZn_2 and containing 290 mOsm sucrose in their aqueous interior, were exposed to a hypotonic solution by diluting polymersome samples 1:1 with deionized water. To track porphyrin emission in PEO_{45}-*b*-PCL_{105} polymersomes, samples of the biodegradable vesicles were incubated at 37 °C and emission spectra were collected over the course of 3 wk. Finally, photoresponsive vesicles containing 500 kDa dextran were prepared as described previously (27).

Hyperspectral Imaging and Spectral Unmixing. Three-dimensional (x, y, λ) image cubes for Fig. 3C and Fig. 4 were collected with a hyperspectral CCD (CRi Nuance FX) camera coupled to an inverted fluorescence microscope (Olympus IX81). The imaging camera has an electronically tunable liquid crystal emission filter that allows collection of emission spectra in nanometer steps across a broad spectral range within seconds to minutes. The time required for image collection depends on the size of the image, emission intensity, and spectral resolution. In our study, the pixel resolution is 0.692 μm/pixel calibrated by a 500-μm width fiduciary using 10X objective. Samples were excited with a mercury lamp with an excitation band-pass filter (530–550 nm). PZn_2 emission was typically collected by the camera from 660 to 720 nm with a 3-nm step size. Spectral unmixing was carried out using the real component analysis method included with the Nuance 2.10 software. Different spectral components in the same image cube were identified and reassigned a pseudocolor in the unmixed image. It was straightforward to subtract any background contribution and obtain an image corresponding to PZn_n emission in different local environments, as established by our fluorometry experiments.

Micropipette Aspiration. Mircopipette aspiration of polymersomes followed similar procedures to those described by Evans and Skalak (30). Both PZn_2-encapsulated (14 mol %) and Nile Red-encapsulated vesicles were picked up by the micropipettes and pressure was increased stepwise in 2–5 cm H_2O increments. The membrane was allowed 10 s after each pressure change to equilibrate. The resulting membrane extensions and membrane diameter were measured with ImageJ software (31) and used to calculate the areal expansion of the different polymersomes ($\Delta A/A_0$). Using the applied pressure, the imposed membrane tension was also calculated. Two methods were used to evaluate spectral changes of porphyrin due to applied membrane stress. First, fluorescence spectra from single polymersomes were obtained through the hyperspectral CCD camera at each applied membrane tension. The dominant emission spectra for each tension, determined by maximum intensity, was used to represent PZn_2 emission. To confirm results, a second, ratiometric method was employed to assess spectral shifts. Light emitted from aspirated polymersomes was spectrally isolated using two band-pass emission filters, HQ690/20 nm and HQ730/20 nm (Chroma Technology), and transmitted to a PMT (Photoscan, Nikon). FeliX software (Photon Technologies) was used to determine the resulting PZn_2 fluorescence intensity. The fluorescence intensity obtained at 690±10 nm was divided by the intensity collected at 730±10 nm to obtain the more twisted/more planar intensity ratio of PZn_2 at each tension applied to the polymersome membrane through aspiration.

ACKNOWLEDGMENTS. We thank Roderic Eckenhoff for assisting the purchase of the Nuance FX camera and Caliper Life Sciences for use of the CRi Nuance EX camera. We thank Eric Johnston for assistance with the photomultiplier tube. This work was supported by National Institutes of Health Grant R01CA115229 (to D.A.H. and M.J.T.) and R01GM083030 (to I.J.D.), the National Science Foundation (NSF) Materials Research Science and Engineering Center program under award DMR05-20020 (to D.A.H., M.J.T., and I.J.D.), and by NSF Grant CHE-0548188, and National Center for Research Resources Award 1S10-RR-021113 (to I.J.D.). N.P.K thanks the NSF for a Graduate Fellowship.

1. Hickenboth CR, et al. (2007) Biasing reaction pathways with mechanical force. *Nature* 446:423–427.
2. Choi CL, Koski KJ, Olson ACK, Alivisatos AP (2010) Luminescent nanocrystal stress gauge. *Proc Natl Acad Sci USA* 107:21306–21310.
3. Kuimova MK, Yahioglu G, Levitt JA, Suhling K (2008) Molecular rotor measures viscosity of live cells via fluorescence lifetime imaging. *J Am Chem Soc* 130:6672–6673.
4. Iio T, Takahashi S, Sawada S (1993) Fluorescent molecular rotor binding to actin. *J Biochem* 113:196–199.
5. Kung CE, Reed JK (1986) Microviscosity measurements of phospholipid-bilayers using fluorescent dyes that undergo torsional relaxation. *Biochemistry* 25:6114–6121.
6. Ghiggino KP, et al. (2007) Porphyrin-based molecular rotors as fluorescent probes of nanoscale environments. *Adv Funct Mater* 17:805–813.
7. Kuimova MK, et al. (2009) Imaging intracellular viscosity of a single cell during photoinduced cell death. *Nat Chem* 1:69–73.
8. Duncan TV, Susumu K, Sinks LE, Therien MJ (2006) Exceptional near-infrared fluorescence quantum yields and excited-state absorptivity of highly conjugated porphyrin arrays. *J Am Chem Soc* 128:9000–9001.
9. Kumble R, Palese S, Lin VSY, Therien MJ, Hochstrasser RM (1998) Ultrafast dynamics of highly conjugated porphyrin arrays. *J Am Chem Soc* 120:11489–11498.
10. Rubtsov IV, Susumu K, Rubtsov GI, Therien MJ (2003) Ultrafast singlet excited-state polarization in electronically asymmetric ethyne-bridged bis (porphinato)Zn(II) complexes. *J Am Chem Soc* 125:2687–2696.
11. Ghoroghchian PP, et al. (2005) Near-infrared-emissive polymersomes: Self-assembled soft matter for in vivo optical imaging. *Proc Natl Acad Sci USA* 102:2922–2927.
12. Ghoroghchian PP, et al. (2006) Quantitative membrane loading of polymer vesicles. *Soft Matter* 2:973–980.
13. Ghoroghchian PP, et al. (2007) Controlling bulk optical properties of emissive polymersomes through intramembranous polymer-fluorophore interactions. *Chem Mater* 19:1309–1318.
14. Duncan TV, Ghoroghchian PP, Rubtsov IV, Hammer DA, Therien MJ (2008) Ultrafast excited-state dynamics of nanoscale near-infrared emissive polymersomes. *J Am Chem Soc* 130:9773–9784.
15. Ghoroghchian PP, et al. (2005) Broad spectral domain fluorescence wavelength modulation of visible and near-infrared emissive polymersomes. *J Am Chem Soc* 127:15388–15390.
16. Forster T, Hoffmann G (1971) Viscosity dependence of fluorescent quantum yields of some dye systems. *Zeitschrift für Physikalische Chemie (Frankfurt)* 75:63–76.
17. Bermudez H, Brannan AK, Hammer DA, Bates FS, Discher DE (2002) Molecular weight dependence of polymersome membrane structure, elasticity, and stability. *Macromolecules* 35:8203–8208.
18. Bermudez H, Aranda-Espiniza H, Hammer DA, Discher DE (2003) Pore stability and dynamics in polymer membranes. *Europhys Lett* 64:550–556.
19. Katz JS, et al. (2009) Membrane stabilization of biodegradable polymersomes. *Langmuir* 25:4429–4434.
20. Katz JS, et al. (2010) Modular synthesis of biodegradable diblock copolymers for designing functional polymersomes. *J Am Chem Soc* 132:3654–3655.
21. Ghoroghchian PP, et al. (2006) Bioresorbable vesicles formed through spontaneous self-assembly of amphiphilic poly(ethylene oxide)-block-polycaprolactone. *Macromolecules* 39:1673–1675.
22. Savic R, Luo L, Eisenberg A, Maysinger D (2003) Micellar nanocontainers distribute to defined cytoplasmic organelles. *Science* 300:615–618.
23. Haag R (2004) Supramolecular drug-delivery systems based on polymeric core-shell architectures. *Angew Chem Int Ed Engl* 43:278–282.
24. Aliabadi HM, Brocks DR, Lavasanifar A (2005) Polymeric micelles for the solubilization and delivery of cyclosporine a: Pharmacokinetics and biodistribution. *Biomaterials* 26:7251–7259.
25. Ahmed F, et al. (2006) Shrinkage of a rapidly growing tumor by drug-loaded polymersomes: pH-triggered release through copolymer degradation. *Mol Pharmaceutics* 3:340–350.
26. Robbins GP, et al. (2009) Photo-initiated destruction of composite porphyrin-protein polymersomes. *J Am Chem Soc* 131:3872–3874.
27. Kamat NP, et al. (2010) A generalized system for photoresponsive membrane rupture in polymersomes. *Adv Funct Mater* 20:2588–2596.
28. Evans E, Needham D (1987) Physical properties of surfactant bilayer membranes: Thermal transitions, elasticity, rigidity, cohesion, and colloidal interactions. *J Phys Chem* 91:4219–4228.
29. Evans EA, Waugh R, Melnik L (1976) Elastic area compressibility modulus of red-cell membrane. *Biophys J* 16:585–595.
30. Evans EA, Skalak R (1979) Mechanics and thermodynamics of biomembranes: Part 1. *CRC Crit Rev Bioeng* 3:181–330.
31. Abramoff MD, Magalhaes PJ, Ram SJ (2004) Image Processing with ImageJ. 11(7) (Biophotonics International), pp 36–42.